

23 **Abstract**

24 Balanced mitochondrial fission and fusion play an important role in shaping and distributing
25 mitochondria, as well as contributing to mitochondrial homeostasis and adaptation to stress. In
26 particular, mitochondrial fission is required to facilitate degradation of damaged or dysfunctional units
27 via mitophagy. Two Parkinson's disease factors, PINK1 and Parkin, are considered key mediators
28 of damage-induced mitophagy, and promoting mitochondrial fission is sufficient to suppress the
29 pathological phenotypes in *Pink1/parkin* mutant *Drosophila*. We sought additional factors that
30 impinge on mitochondrial dynamics and which may also suppress *Pink1/parkin* phenotypes. We
31 found that the *Drosophila* phosphatidylinositol 4-kinase III β homologue, Four wheel drive (Fwd),
32 promotes mitochondrial fission downstream of the pro-fission factor Drp1. Previously described only
33 as male sterile, we identified several new phenotypes in *fwd* mutants, including locomotor deficits
34 and shortened lifespan, which are accompanied by mitochondrial dysfunction. Finally, we found that
35 *fwd* overexpression can suppress locomotor deficits and mitochondrial disruption in *Pink1/parkin*
36 mutants, consistent with its function in promoting mitochondrial fission. Together these results shed
37 light on the complex mechanisms of mitochondrial fission and further underscore the potential of
38 modulating mitochondrial fission/fusion dynamics in the context of neurodegeneration.

39

40 **Author Summary**

41 Mitochondria are dynamic organelles that can fuse and divide, in part to facilitate turnover of
42 damaged components. These processes are essential to maintain a healthy mitochondrial network,
43 and, in turn, maintain cell viability. This is critically important in high-energy, post-mitotic tissues such
44 as neurons. We previously identified *Drosophila* phosphatidylinositol-4 kinase *fwd* as a pro-fission
45 factor in a cell-based screen. Here we show that loss of *fwd* regulates mitochondrial fission *in vivo*,
46 and acts genetically downstream of *Drp1*. We identified new phenotypes in *fwd* mutants, similar to
47 loss of *Pink1/parkin*, two genes linked to Parkinson's disease and key regulators of mitochondrial
48 homeostasis. Importantly, *fwd* overexpression is able to substantially suppress locomotor and
49 mitochondrial phenotypes in *Pink1/parkin* mutants, suggesting manipulating phosphoinositides may
50 represent a novel route to tackling Parkinson's disease.

51

52 **Introduction**

53 Mitochondria are dynamic organelles that are transported to the extremities of the cell and frequently
54 undergo fusion and fission events, which influences their size, branching and degradation. Many of
55 the core components of the mitochondrial fission and fusion machineries have been well
56 characterised, these include the pro-fusion factors Mfn1/2 and Opa1, and pro-fission factors Drp1
57 and Mff (1). Maintaining an appropriate balance of fission and fusion, as well as transport dynamics,
58 is crucial for cellular health and survival as mutations in many of the core components cause severe
59 neurological conditions in humans and model organisms (2).

60 The mitochondrial fission/fusion cycle has been linked to the selective removal of damaged
61 mitochondria through the process of autophagy (termed mitophagy), in which defective mitochondria
62 are engulfed into autophagosomes and degraded by lysosomes (3, 4). Two genes that have been
63 firmly linked to the mitophagy process are *PINK1* and *PRKN* (5-7). Mutations in these genes cause
64 autosomal-recessive juvenile parkinsonism, associated with degeneration of midbrain dopaminergic
65 neurons and motor impairments, among other symptoms and pathologies. Studies from a wide
66 variety of model systems have shown various degrees of mitochondrial dysfunction associated with
67 mutation of *PINK1/PRKN* homologues including disrupted fission/fusion (8-16). *Drosophila* have
68 proven to be a fruitful model for investigating the function of the conserved homologues *Pink1* and
69 *parkin*, with these mutants exhibiting robust mitochondrial disruption and neuromuscular
70 phenotypes. Importantly, several studies have shown that the pathological consequences of loss of
71 *Pink1* or *parkin* can be largely suppressed by genetic manipulations that increase mitochondrial
72 fission or reduce fusion (17-23).

73 To identify genes involved in mitochondrial quality control and homeostasis, we previously
74 performed an RNAi screen in *Drosophila* S2 cells to identify kinases and phosphatases that
75 phenocopy or suppress hyperfused mitochondria caused by loss of *Pink1* (24). We identified the
76 phosphatidylinositol 4-kinase III β homologue, *four wheel drive* (*fwd*), whose knockdown
77 phenocopied *Pink1* RNAi, resulting in excess mitochondrial fusion. *Drosophila* mutant for *fwd* have
78 been reported to be viable but male sterile due to incomplete cytokinesis during spermatogenesis
79 (25-28); however, no other organismal phenotypes or mitochondrial involvement have been

80 described to date. Thus, we sought to better understand the role of *Fwd* in mitochondrial
81 homeostasis.

82 In this study, we have characterised *fwd* mutants for organismal phenotypes associated with
83 *Pink1/parkin* dysfunction, and analysed the impact on mitochondrial form and function. We have
84 also investigated genetic interactions between *fwd* and *Pink1/parkin*, as well as with mitochondrial
85 fission/fusion factors. We found that loss of *fwd* inhibited mitochondrial function, causing increased
86 mitochondrial length and branching, and decreased respiratory capacity. These effects were
87 associated with shortened lifespan and dramatically reduced locomotor ability, similar to *Pink1* and
88 *parkin* mutants. Furthermore, *fwd* overexpression was sufficient to significantly suppress
89 *Pink1/parkin* mutant locomotor deficits and mitochondrial phenotypes. Interestingly, we found that
90 the mitochondrial and locomotion phenotypes in *fwd* mutants can be rescued by loss of pro-fusion
91 factors *Marf* and *Opa1*, but the activity of *Drp1* appears to require *fwd*. These results support a role
92 for *fwd* in regulating mitochondrial morphology, specifically in facilitating mitochondrial fission, and
93 further substantiate the important contribution of aberrant mitochondrial fission/fusion dynamics in
94 *Pink1/parkin* phenotypes.

95

96 **Results**

97 **Loss of *fwd* causes mitochondrial hyperfusion along with locomotor and lifespan deficits**

98 We previously found that knockdown of *fwd* phenocopied loss of *Pink1* in cultured cells by causing
99 mitochondrial hyperfusion (24). To extend these *in vitro* observations we sought to determine
100 whether *fwd* has a broader role in regulating mitochondrial homeostasis *in vivo*. In striking similarity
101 to *Pink1* mutants, mutations in *fwd* have previously been shown to cause male sterility due to
102 aberrant spermatogenesis (25-28); however, no other organismal phenotypes have been described.

103 *Pink1* mutants have a range of additional phenotypes including deficits in negative geotaxis
104 (climbing ability), disruption of flight muscle mitochondria, shortened lifespan, and modest
105 degeneration of dopaminergic (DA) neurons (10, 29). Thus, we assessed these phenotypes in two
106 *fwd* mutants – a nonsense mutation, *fwd*³, and a *P*-element insertion, *fwd*^{neo1}. In all instances, these
107 mutations were crossed to a deficiency (*Df(3L)7C*) to avoid potential extragenic effects from

108 homozygosity. Both mutant combinations, fwd^{β}/Df and fwd^{neo1}/Df (hereafter, designated simply as
109 fwd^{β} and fwd^{neo1}), displayed a striking loss of climbing ability in young flies (Fig. 1A), though the
110 phenotype was weaker in fwd^{neo1} consistent with it being a hypomorph. Notably, transgenic re-
111 expression of fwd using a ubiquitous driver ($da-GAL4$), was able to restore climbing ability to near
112 wild-type levels (Fig. 1A), supporting the specificity of this phenotype for loss of fwd . Analysing
113 longevity in the fwd^{β} null mutants, revealed a significant reduction in median lifespan (Fig. 1B).
114 However, no significant loss of DA neurons was detected in aged fwd mutant brains (Fig. 1C). These
115 results reveal some phenotypic similarity between *Pink1* and fwd mutants at the organismal level as
116 well as the cellular level.

117 To investigate the relative contribution of fwd to locomotor ability in different tissues, we
118 expressed a transgenic RNAi construct (30) via tissue-specific drivers. We first verified that
119 ubiquitous knockdown of fwd via $da-GAL4$ phenocopied the genetic mutants, thus, demonstrating
120 its efficacy to recapitulate null mutant phenotypes (Fig. 1D). Interestingly, pan-neuronal knockdown,
121 using $nSyb-GAL4$, reproduced the striking loss of climbing ability, whereas knockdown in all muscles
122 via $Mef2-GAL4$ only modestly affected climbing (Fig. 1D). Thus, fwd shows some tissue-selective
123 requirement but plays an important role in the nervous system that was not previously appreciated.

124 Since fwd knockdown in cultured cells caused mitochondrial fusion, similar to loss of *Pink1*,
125 we sought to further characterise the impact of fwd loss on mitochondria *in vivo*. Mitochondria are
126 particularly abundant in adult flight muscles, and this tissue is severely affected in *Pink1/parkin*
127 mutants (8, 10, 29), so we first analysed mitochondrial morphology in fwd mutants in this tissue.
128 Imaging mitochondria by fluorescence or electron-microscopy in flight muscles revealed them to be
129 grossly normal in their cristae structure, size and abundance compared to control (Fig. 2A-B).

130 We next sought to analyse the mitochondrial morphology in a tissue where the specific
131 knockdown of fwd resulted in strong climbing defects. We analysed the network morphology in cell
132 bodies of the larval ventral ganglion (part of the central nervous system). Expression of mitoGFP in
133 a subset of neurons, driven by $CCAP-GAL4$, allowed better three-dimensional imaging of the
134 mitochondrial network (Fig. 2C). While the overall appearance was similar between fwd mutant and
135 control, quantitative analysis of the networks revealed that both the length and connectivity (number

136 of branches) were increased upon loss of *fwd* (Fig. 2D-F). These results are consistent with the
137 previous cell-based study indicating loss of *fwd* causes mitochondrial hyperfusion.

138 We next assessed mitochondrial function, analysing maximal respiratory capacity in intact
139 mitochondria and overall ATP levels in whole animals. Respiration measured by the oxygen
140 consumption rate in energised mitochondria, stimulated via either complex I or complex II substrates,
141 was significantly reduced in *fwd* mutants (Fig. 3A). However, the overall level of ATP was not
142 significantly affected (Fig. 3B). These results indicate that mitochondrial respiration is affected by
143 loss of *fwd* but compensatory mechanisms could still maintain normal steady-state ATP levels in the
144 organism.

145 146 ***fwd* mutant phenotypes are suppressed by loss of fusion factors**

147 The results above substantiate that loss of *fwd* causes excess mitochondrial fusion *in vivo*. We next
148 addressed whether the mitochondrial hyperfusion may contribute to the locomotor deficit. To do this
149 we combined ubiquitous expression of *fwd* RNAi with genetic manipulations that reduce fusion
150 (partial loss of pro-fusion factors *Marf* or *Opa1*) or promote fission (overexpression of pro-fission
151 factor *Drp1*), and assessed climbing behaviour. Heterozygous loss of either *Marf* (the fly homologue
152 of *MFN1/2*) or *Opa1*, which did not affect climbing alone, was sufficient to significantly suppress the
153 climbing deficit caused by *fwd* RNAi (Fig. 4A, B). However, contrary to what we expected,
154 overexpression of *Drp1* was not able to ameliorate the climbing defect (Fig. 4C).

155 To better understand these results, we analysed the mitochondrial morphology in neuronal
156 cell bodies of these genotypes. As with the *fwd* mutant, *fwd* RNAi caused a significant elongation of
157 mitochondria and increased branching (Fig. 4D-F). Consistent with the effects on climbing,
158 heterozygous loss of *Marf* or *Opa1* reverted the increase in mitochondrial length, whereas *Drp1*
159 overexpression did not (Fig. 4D, E). Interestingly, the increased branching caused by loss of *fwd*
160 was suppressed by heterozygous loss of *Marf* or *Drp1* overexpression, but not by heterozygous loss
161 of *Opa1* (Fig. 4D, F). The reasons for the complex effects on branching are unclear but may reflect
162 that *Marf* directs fusion of the OMM (and hence, coordinates branching), while *Opa1* regulates fusion
163 of IMM. Nevertheless, the effects on mitochondrial branch length suggest that *Drp1* may require
164 *Fwd* to execute mitochondrial fission. Overall, the genetic interaction of *Marf* and *Opa1* suppressing

165 the *fwd* RNAi-induced climbing deficit supports this phenotype being, at least partially, caused by
166 mitochondrial hyperfusion.

167
168 ***fwd* overexpression can suppress *Pink1/parkin* mutant phenotypes**

169 While many studies have focused on the role of PINK1/Parkin in damage-induced mitophagy,
170 aberrant mitochondrial dynamics is clearly a major cause of *Pink1/parkin* mutant phenotypes in
171 *Drosophila*, including locomotor deficits and flight muscle degeneration, since these can be
172 substantially suppressed by promoting mitochondrial fission (17-20). As our results indicate that Fwd
173 promotes mitochondrial fission, we next tested whether overexpression of *fwd* could ameliorate
174 *Pink1* and *parkin* mutant phenotypes. Combining *Pink1/parkin* mutants with ubiquitous *fwd*
175 overexpression was sufficient to significantly suppress the climbing deficit in both mutants (Fig. 5A,
176 B). In addition, the thoracic indentations caused by degeneration of the underlying flight muscle were
177 also significantly improved (Fig. 5C). Disruption of mitochondrial integrity in the flight muscles was
178 also visibly improved when *fwd* was overexpressed in muscles (Fig. 5D). These results are
179 consistent with Fwd overexpression promoting mitochondrial fission and partially reverting the
180 hyperfusion caused by *Pink1/parkin* loss.

181
182 We were intrigued by the earlier observation that heterozygous loss of *Marf* or *Opa1* could
183 revert the aberrant mitochondrial morphology and climbing defect of *fwd* RNAi, but the
184 overexpression of *Drp1* did not (Fig. 4). These results suggested that the activity of Drp1 might
185 require Fwd, which we sought to test further. As a paradigm for Drp1 activity, overexpression of *Drp1*
186 is sufficient to substantially suppress the climbing deficit and mitochondrial disruption in *Pink1* and
187 *parkin* mutants (Fig. 6A-D), as previously reported (18). Remarkably, coincident knockdown of *fwd*
188 completely prevented the ability of Drp1 to rescue the *Pink1/parkin* mutant phenotypes (Fig. 6A-D).
189 These results further indicates that Drp1 requires the activity of Fwd.

190

191 Discussion

192 We previously identified knockdown of *fwd* to induce mitochondrial hyperfusion in cultured cells,
193 similar to loss of *Pink1* (24). Here we have validated that genetic loss or knockdown of *fwd* also
194 causes excess mitochondrial fusion in neuronal cells *in vivo*, leading to increased mitochondrial
195 length and branching (Fig. 2). As mitochondrial fission/fusion dynamics have been shown to be
196 important for proper mitochondrial homeostasis (2), it is not surprising that this also has an impact
197 on respiration at the organismal level (Fig. 3). Furthermore, it follows that this in turn has an impact
198 on organismal fitness and vitality (Fig. 1). While *fwd* mutants have previously been shown to be male
199 sterile, we describe for the first time new phenotypes associated with loss of *fwd*: profound locomotor
200 deficits and shortened lifespan. Interestingly, there is a stronger requirement for *fwd* in the nervous
201 system compared to the musculature.

202 The robust locomotor phenotype allowed us to test the genetic relationship between *fwd* and
203 core components of the mitochondrial fission/fusion machinery. Given the excess mitochondrial
204 fusion in *fwd* mutants, suppression of the organismal phenotypes by reduction of fusion factors *Marf*
205 and *Opa1* was expected. However, it was surprising that overexpression of the fission factor *Drp1*
206 was unable to ameliorate organismal phenotypes or even the mitochondrial morphology (Fig. 4).
207 These results suggested that *Drp1* requires *Fwd* to function. Consistent with this, *Drp1*
208 overexpression was no longer able to rescue *Pink1/parkin* mutant phenotypes in the absence of *fwd*
209 (Fig. 6). These genetic experiments strongly hint at a functional link between *Drp1* and *Fwd* but do
210 not illuminate the molecular mechanism underpinning it. *Fwd*, is the *Drosophila* homologue of
211 phosphatidylinositol 4-kinase III β [PI(4)KB], which mediates the phosphorylation of
212 phosphatidylinositol to generate phosphatidylinositol 4-phosphate [PI(4)P] (31). PI(4)P is one of the
213 most abundant phosphoinositides, which is usually concentrated in the trans-Golgi network (32);
214 thus, an obvious mechanism by which PI(4)P may influence mitochondrial dynamics is not
215 immediately apparent. However, while this manuscript was in preparation, Nagashima and
216 colleagues reported that Golgi-derived PI(4)P-containing vesicles were required for the final stages
217 of mitochondrial fission (33). In that study, the authors found that loss of PI(4)KIII β led to a
218 hyperfused and branched mitochondrial network, consistent with what we observed here (Fig. 2).
219 Moreover, they described that while *Drp1* was still recruited, it was unable to fully execute the

220 scission event, although the reason is unclear, leading to extended mitochondrial constriction sites.
221 Our genetic evidence that the action of Drp1 requires Fwd is consistent with these findings, and
222 provide an *in vivo* validation of Nagashima and colleagues' results. Further, it is interesting to note
223 that while the study by Nagashima et al. suggests a universal role for PI(4)P in mitochondrial fission,
224 our *in vivo* analysis revealed that while *fwd* affected mitochondrial morphology in the nervous
225 system, it appeared to have no major impact in the musculature. These tissue-specific requirements
226 were borne out in the strong locomotor deficits caused by neuronal loss of *fwd* but much less so by
227 knockdown in muscles. Clearly, further work is required to better understand the complexities of
228 regulated fission/fusion events in different cell contexts *in vivo*.

229 A key role of mitochondrial fission/fusion dynamics is in contributing to a quality control
230 mechanism of mitochondrial sorting to eliminate dysfunctional units via mitophagy (3, 4). A
231 substantial body of evidence from cellular models indicates that mammalian PINK1/Parkin act to
232 promote damage-induced mitophagy (5-7), and some *in vivo* evidence from *Drosophila* also
233 supports this (34, 35). However, the precise nature of PINK1/Parkin-mediated mitochondrial
234 turnover *in vivo* is debated with contradictory results emerging (36-40). Nevertheless, interventions
235 to combat the decline in mitochondrial homeostasis remain a key challenge to combatting
236 *PINK1/PRKN* related pathologies. One mechanism that seems to provide substantial benefit in
237 physiological contexts is through augmenting mitochondrial fission, which presumably facilitates the
238 flux of damaged mitochondrial components towards turnover (17-20). Here, we provide further
239 evidence that augmenting a pro-fission pathway is beneficial against *Pink1/parkin* dysfunction. As
240 phosphoinositides can be interconverted by the action of multiple enzymes that may be druggable,
241 these findings suggest another potential route towards a therapeutic intervention.

242

243 **Methods**

244 ***Drosophila* stocks and husbandry**

245 Flies were raised and kept under standard conditions in a temperature-controlled incubator with a
246 12h:12h light:dark cycle at 25 °C and 65% relative humidity, on food consisting of agar, cornmeal,
247 molasses, propionic acid and yeast. The following strains were obtained from the Bloomington
248 *Drosophila* Stock Center (RRID:SCR_006457): *w*¹¹¹⁸ (RRID:BDSC_6326), *fwd*^{neo1}
249 (RRID:BDSC_10069), *Df(3L)7C* (RRID:BDSC_5837), *Opa1*^{s3475} (RRID:BDSC_12188), *da-GAL4*
250 (RRID:BDSC_55850), *nSyb-GAL4* (RRID:BDSC_51941), *Mef2-GAL4* (RRID:BDSC_27390),
251 *CCAP-GAL4* (RRID:BDSC_25685, RRID:BDSC_25686), *UAS-mito-HA-GFP* (RRID:BDSC_8442,
252 RRID:BDSC_8443), *fwd*^{RNAi} (RRID:BDSC_35257), *luciferase*^{RNAi} (RRID:BDSC_31603). Other lines
253 were kindly provided as follows: *fwd*³ from J. Brill (27), and the *Pink1*^{B9} and *UAS-Drp1* from J. Chung
254 (10), *Mar*^B from H. Bellen (41). The *park*²⁵ mutants have been described previously (8). *UAS-GFP-*
255 *fwd* was generated by PCR amplification of the GFP-*fwd* sequence from a *hsp83::GFP-fwd* plasmid
256 (28), kindly provided by G. Polevoy and J. Brill, and cloned into pUAST.attB for integration at the
257 attP40 locus (BestGene Inc.). All experiments in adult flies were conducted using males, except Fig.
258 4A where females were used.

259

260 **Locomotor assays**

261 The startle induced negative geotaxis (climbing) assay was performed using a counter-current
262 apparatus. Experiments were performed using 2-3 days old flies. Except for figure 4A, all the
263 climbing assays used males. Briefly, 20-23 flies were placed into the first chamber, tapped to the
264 bottom, and given 10 s to climb a 10 cm distance. This procedure was repeated five times (five
265 chambers), and the number of flies that has remained into each chamber counted. The weighted
266 performance of several group of flies for each genotype was normalized to the maximum possible
267 score and expressed as *Climbing index* (8).

268

269 **Lifespan**

270 For lifespan experiments, flies were grown under identical conditions at low density. Progeny were
271 collected under very light anaesthesia and kept in tubes of approximately 25 males each, and

272 transferred every 2-3 days to fresh media and the number of dead flies recorded. Percent survival
273 was calculated at the end of the experiment after correcting for any accidental loss.

274

275 **Immunohistochemistry and sample preparation**

276 For immunostaining, adult flight muscles were dissected in PBS and fixed in 4% formaldehyde for
277 30 min at RT, permeabilized in 0.3% Triton X-100 for 30 min, and blocked with 0.3% Triton X-100
278 plus 4% Horse Serum (HS) in PBS for 1 h at RT. Tissues were incubated with ATP5A antibody
279 (Abcam Cat# ab14748, RRID:AB_301447; 1:500), diluted in 0.3% Triton X-100 plus 4% HS in PBS
280 overnight at 4°C, then rinsed 3 times 10 min with 0.3% Triton X-100 in PBS, and incubated with the
281 appropriate fluorescent secondary antibodies overnight at 4°C. The tissues were washed 2 times in
282 PBS and mounted on slides. Adult brains were dissected in PBS and fixed on ice in 4% formaldehyde
283 for 30 min, permeabilized in 0.3% Triton X-100 for 30 min, and blocked with 0.3% Triton X-100 plus
284 4% HS in PBS for 4 h at RT. Incubation with Tyrosine Hydroxylase Antibody (TH) antibody
285 (Immunostar Cat#22941, 1:200) diluted in 0.3% Triton X-100 plus 4% HS was done for 72h at 4°C.
286 Secondary antibody was incubated for 3 h at RT. Then washes were done 3 times for 20 min with
287 0.3% Triton X-100 in PBS and mounted in carved slides. Larvae brains were dissected on PBS and
288 mounted sideways on slides coated with poly-lysine at 0.9 mg/ml . They were fixed in 4%
289 formaldehyde for 20 min at RT, then washed in PBS. All the sample preparations were mounted
290 using Prolong Diamond Antifade mounting medium (Thermo Fischer Scientific Cat# P36961).

291

292 **Microscopy**

293 Fluorescence imaging was conducted using a Zeiss LSM 880 confocal microscope (Carl Zeiss
294 MicroImaging) equipped with Nikon Plan-Apochromat 100x/1.4 NA oil immersion objectives. Images
295 were taken at a resolution of 2048x2048 pixels and they were prepared using Fiji software
296 (RRID:SCR_002285).

297

298 **Analysis of mitochondrial morphology**

299 Motoneuron cell bodies from larvae ventral nerve cord expressing *CCAP-GAL4* were used to
300 analyse mitochondrial branches marked by mitoGFP. All images were processed using Fiji software
301 (RRID:SCR_002285). Z-stacks of individual neurons were cropped to a size of 232×232 pixels. The
302 mitoGFP signal was enhanced and smoothed using two filters: unsharp mask (radius =10.0 pixels,
303 Mask strength 0.9) and median filtering (radius =3). Then binary masks were created using “Otsu
304 method” in auto and Dark background, and ‘skeletonized’ from the Process and Binary menu served
305 to generate the branches. These skeletonized images were analysed using Analyse Skeleton
306 (2D/3D). Finally, Median branch length per cell was calculated using Branch Length column from
307 “Branch information” window, and the proportion of individual vs interconnected branches per cell
308 was calculated by taking the “Number of branches” column from the “Results” window.

309

310 **Transmission electron-microscopy**

311 Thoraces were prepared from 5-day-old adult flies and treated as previously described (8). Ultra-
312 thin sections were examined using a FEI Tecnai G2 Spirit 120KV transmission electron-microscope.

313

314 **Respirometry analysis**

315 Respiration was monitored at 30 °C using an Oxygraph-2k high-resolution respirometer
316 (OROBOROS Instruments) using a chamber volume set to 2 mL. Calibration with air-saturated
317 medium was performed daily. Data acquisition and analysis were carried out using Datlab software
318 (OROBOROS Instruments). Five flies per genotype (equal weight) were homogenised in respiration
319 buffer (120 mM sucrose, 50 mM KCl, 20 mM Tris-HCl, 4 mM KH₂PO₄, 2 mM MgCl₂, and 1 mM EGTA,
320 1 g/l fatty acid-free BSA, pH 7.2). For coupled (state 3) assays, complex I-linked respiration was
321 measured at saturating concentrations of malate (2 mM), glutamate (10 mM) and adenosine
322 diphosphate (ADP, 2.5 mM). Complex II-linked respiration was assayed in respiration buffer
323 supplemented with 0.15 μM rotenone, 10 mM succinate and 2.5 mM ADP. Data from 7-8
324 independent experiments were averaged.

325

326 **ATP levels**

327 The ATP assay was performed as described previously (24). Briefly, five male flies for each
328 genotype were homogenized in 100 μ L 6 M guanidine-Tris/EDTA extraction buffer and subjected to
329 rapid freezing in liquid nitrogen. Homogenates were diluted 1/100 with the extraction buffer and
330 mixed with the luminescent solution (CellTiter-Glo Luminescent Cell Viability Assay, Promega).
331 Luminescence was measured with a SpectraMax Gemini XPS luminometer (Molecular Devices).
332 The average luminescent signal from technical triplicates was expressed relative to protein levels,
333 quantified using the Pierce BCA Protein Assay kit (ThermoFisher Scientific). Data from 3
334 independent experiments were averaged and the luminescence expressed as a percentage of the
335 control.

336

337 **Statistical analysis**

338 Data from the various experimental assays were analysed as follows: For behavioural analyses,
339 Kruskal-Wallis non-parametric test with Dunn's post-hoc correction for multiple comparisons was
340 used. Lifespan was analysed by Log-rank (Mantel-Cox) test. Categorical analyses (i.e. thoracic
341 indentations) were analysed by Chi-square test. Mitochondrial branch length by Mann-Whitney non-
342 parametric test, and connectivity by Kruskal-Wallis with Dunn's post-hoc correction. ATP levels were
343 analysed by unpaired *t*-test, and respiration by paired *t*-test. Analyses were performed using
344 GraphPad Prism 8 software (RRID:SCR_002798) and RStudio software (RRID:SCR_000432).

345

346

347 **Data availability**

348 All data that support the findings of this study are available on reasonable request to the
349 corresponding author. The contributing authors declare that all relevant data are included in the
350 paper.

351

352

353 **Acknowledgements**

354 This work is supported by MRC core funding (MC_UU_00015/4, MC-A070-5PSB0 and
355 MC_UU_00015/6) and ERC Starting grant (DYNAMITO; 309742). Stocks were obtained from the
356 Bloomington *Drosophila* Stock Center which is supported by grant NIH P40OD018537. We thank J.
357 Brill for sharing *fwd* stocks, Claire Pilgrim for technical assistance, and J. Prudent for sharing results
358 prior to publication. We thank members of the Whitworth lab for fruitful discussions and feedback on
359 the manuscript.

360

361

362 **Author Contributions**

363 A.T-F. and E.L.W. designed and performed experiments, and analysed data. A.J.W. conceived the
364 study, designed experiments, analysed the data and supervised the work. A.J.W. wrote the
365 manuscript with input from all authors.

366

367

368 **Declaration of interest**

369 The authors declare no competing interests.

370

371 **Figure Legends**

372 **Figure 1. Loss of *fwd* causes motor deficits and shortened lifespan.**

373 (A) Climbing assay of *fwd* mutants (*fwd*^β and *fwd*^{neo1}) in trans to a deficiency (Df), alone or with
374 transgenic overexpression of *fwd* (*fwd* O/E) driven by *da-GAL4*. (B) Lifespan analysis of control and
375 *fwd* mutants. Significance for lifespan was analysed by log-rank (Mantel-Cox) test. (C) Quantification
376 of dopaminergic neurons in PPL1 cluster of 30-day-old adult brains. Chart shows mean ± SD with
377 individual data points. Significance was analysed by Mann-Whitney test. (D) Climbing analysis of
378 *fwd* knockdown (RNAi) in all (ubiquitous) or selected tissues. Charts show mean ± 95% confidence
379 interval (CI); number of animals analysed is shown in each bar. Significance for climbing was
380 analysed by Kruskal-Wallis test with Dunn's post-hoc correction for multiple comparisons.
381 Comparison is against the control unless otherwise indicated; * $P < 0.05$, *** $P < 0.001$, **** $P < 0.0001$;
382 ns, non-significant. Full genotypes are given in Supplementary Table 1.

383

384 **Figure 2. Loss of *fwd* causes excess mitochondrial fusion.**

385 (A) Confocal microscopy analysis of mitochondrial morphology, visualised using mitoGFP, in control
386 and *fwd* mutant flight muscles. Scale bar = 10 μm. (B) Electron-microscopy analysis of mitochondrial
387 structure in flight muscles. Scale bar = 1 μm. (C) Confocal microscopy analysis of mitochondrial
388 network morphology (mitoGFP) in neuronal cell bodies from larval ventral ganglion of control and
389 *fwd* mutants. Image shows a projected z-stack. Scale bar = 2 μm. (C') Skeletonised image of
390 mitochondrial network used for quantification. (D) Quantification of median mitochondrial branch
391 length per cell. Violin plot indicating median (thick, horizontal line) and quartiles (dashed lines).
392 Significance was analysed by Mann-Whitney test. (E) Frequency distribution plot of mitochondrial
393 network connectivity (number of branches) per cell. N = 46 (control) and 54 (*fwd*). (F) Chart
394 summarising quantification of connectivity shown in E, plotting the proportion of individual
395 mitochondria (0 branches) and connected mitochondria (1-10 branches) relative to the total number
396 of networks per cell. Significance was analysed by Kruskal-Wallis test with Dunn's post-hoc
397 correction for multiple comparisons. * $P < 0.05$, ** $P < 0.01$. Full genotypes are given in Supplementary
398 Table 1.

399

400 **Figure 3. Loss of *fwd* inhibits mitochondrial respiration.**

401 (A) Mitochondrial respiration analysis by oxygen consumption rate (OCR) and (B) ATP levels in
402 control and *fwd* mutant adults. Charts show mean \pm SEM. Significance was analysed by paired (A)
403 or unpaired (B) *t*-test. * $P < 0.05$; ns, non-significant. Full genotypes are given in Supplementary Table
404 1.

405

406 **Figure 4. *fwd* genetically interacts with mitochondrial fission/fusion factors.**

407 (A-C) Climbing assay of *fwd* RNAi alone or in combination with heterozygous *Marf* or *Opa1* mutations
408 or transgenic overexpression of *Drp1*. Transgenic expression was mediated via *da-GAL4*. Charts
409 show mean \pm 95% confidence interval (CI); number of animals analysed is shown in each bar. (D)
410 Confocal microscopy analysis of mitochondrial network morphology (mitoGFP) in neuronal cell
411 bodies from larval ventral ganglion of control, *fwd* RNAi alone and in combination with heterozygous
412 *Marf* or *Opa1* mutations or transgenic overexpression of *Drp1*. Image shows a projected z-stack.
413 Scale bar = 2 μ m. (D') Skeletonised image of mitochondrial network used for quantification. (E)
414 Quantification of median mitochondrial branch length per cell. Violin plot indicating median (thick,
415 horizontal line) and quartiles (dashed lines). Significance was analysed by Mann-Whitney test. (F)
416 Plot of the proportion of individual mitochondria (0 branches) and connected mitochondria (1-10
417 branches) quantified per cell. Significance was calculated by Kruskal-Wallis test with Dunn's post-
418 hoc correction for multiple comparisons. Comparison is against the control unless otherwise
419 indicated; * $P < 0.05$, *** $P < 0.001$, **** $P < 0.0001$; ns, non-significant. Full genotypes are given in
420 Supplementary Table 1.

421

422 **Figure 5. *fwd* overexpression partially suppresses *Pink1/parkin* phenotypes.**

423 (A, B) Climbing assay of control, *Pink1* or *parkin* mutants with or without *fwd* overexpression induced
424 by *da-GAL4*. Significance was analysed by Kruskal-Wallis test with Dunn's post-hoc correction for
425 multiple comparisons. Comparison is against the control unless otherwise indicated; * $P < 0.05$, ***
426 $P < 0.001$, **** $P < 0.0001$; ns, non-significant. (C) Analysis of thoracic indentations evident in *Pink1* or
427 *parkin* mutants in the presence of absence of *fwd* overexpression, induced by *da-GAL4*. Significance

428 was determined by Chi-squared test. **** $P < 0.0001$. (D) Confocal microscopy analysis of
429 mitochondrial integrity, visualised by anti-ATP5A immunostaining, in flight muscles of the indicated
430 genotypes. Transgenic expression was mediated via *Mef2-GAL4*. Scale bar = 10 μm . Full genotypes
431 are given in Supplementary Table 1.

432

433 **Figure 6. *Drp1* activity requires *fwd* in suppressing *Pink1/parkin* phenotypes.**

434 (A, B) Climbing assay of control, *Pink1* or *parkin* mutants with or without *Drp1* overexpression or
435 concomitant induction of *fwd* RNAi. Significance was analysed by Kruskal-Wallis test with Dunn's
436 post-hoc correction for multiple comparisons. Comparison is against the control unless otherwise
437 indicated; ** $P < 0.01$, *** $P < 0.001$, **** $P < 0.0001$; ns, non-significant. (C, D) Confocal microscopy
438 analysis of mitochondrial integrity, visualised by anti-ATP5A immunostaining, in flight muscles of the
439 indicated genotypes. For all conditions, transgenic expression was mediated via *da-GAL4*. Scale
440 bar = 10 μm . Full genotypes are given in Supplementary Table 1.

441

442 **References**

- 443 1. Tilokani L, Nagashima S, Paupe V, Prudent J. Mitochondrial dynamics: overview of
444 molecular mechanisms. *Essays Biochem.* 2018;62(3):341-60.
- 445 2. Nunnari J, Suomalainen A. Mitochondria: in sickness and in health. *Cell.* 2012;148(6):1145-
446 59.
- 447 3. Twig G, Hyde B, Shirihai OS. Mitochondrial fusion, fission and autophagy as a quality control
448 axis: the bioenergetic view. *Biochim Biophys Acta.* 2008;1777(9):1092-7.
- 449 4. Twig G, Shirihai OS. The interplay between mitochondrial dynamics and mitophagy. *Antioxid*
450 *Redox Signal.* 2011;14(10):1939-51.
- 451 5. McWilliams TG, Muqit MM. PINK1 and Parkin: emerging themes in mitochondrial
452 homeostasis. *Curr Opin Cell Biol.* 2017;45:83-91.
- 453 6. Nguyen TN, Padman BS, Lazarou M. Deciphering the Molecular Signals of PINK1/Parkin
454 Mitophagy. *Trends Cell Biol.* 2016;26(10):733-44.
- 455 7. Pickrell AM, Youle RJ. The roles of PINK1, parkin, and mitochondrial fidelity in Parkinson's
456 disease. *Neuron.* 2015;85(2):257-73.
- 457 8. Greene JC, Whitworth AJ, Kuo I, Andrews LA, Feany MB, Pallanck LJ. Mitochondrial
458 pathology and apoptotic muscle degeneration in *Drosophila* parkin mutants. *Proceedings of the*
459 *National Academy of Sciences of the United States of America.* 2003;100(7):4078-83.
- 460 9. Palacino JJ, Sagi D, Goldberg MS, Krauss S, Motz C, Wacker M, et al. Mitochondrial
461 dysfunction and oxidative damage in parkin-deficient mice. *The Journal of biological chemistry.*
462 2004;279(18):18614-22.
- 463 10. Park J, Lee SB, Lee S, Kim Y, Song S, Kim S, et al. Mitochondrial dysfunction in *Drosophila*
464 PINK1 mutants is complemented by parkin. *Nature.* 2006;441(7097):1157-61.
- 465 11. Mortiboys H, Thomas KJ, Koopman WJ, Klaffke S, Abou-Sleiman P, Olpin S, et al.
466 Mitochondrial function and morphology are impaired in parkin-mutant fibroblasts. *Ann Neurol.*
467 2008;64(5):555-65.
- 468 12. Exner N, Treske B, Paquet D, Holmstrom K, Schiesling C, Gispert S, et al. Loss-of-function
469 of human PINK1 results in mitochondrial pathology and can be rescued by parkin. *J Neurosci.*
470 2007;27(45):12413-8.

- 471 13. Gautier CA, Kitada T, Shen J. Loss of PINK1 causes mitochondrial functional defects and
472 increased sensitivity to oxidative stress. *Proceedings of the National Academy of Sciences of the*
473 *United States of America*. 2008;105(32):11364-9.
- 474 14. Flinn L, Mortiboys H, Volkmann K, Koster RW, Ingham PW, Bandmann O. Complex I
475 deficiency and dopaminergic neuronal cell loss in parkin-deficient zebrafish (*Danio rerio*). *Brain*.
476 2009;132(Pt 6):1613-23.
- 477 15. Morais VA, Verstreken P, Roethig A, Smet J, Snellinx A, Vanbrabant M, et al. Parkinson's
478 disease mutations in PINK1 result in decreased Complex I activity and deficient synaptic function.
479 *EMBO Mol Med*. 2009;1(2):99-111.
- 480 16. Grunewald A, Gegg ME, Taanman JW, King RH, Kock N, Klein C, et al. Differential effects
481 of PINK1 nonsense and missense mutations on mitochondrial function and morphology. *Exp Neurol*.
482 2009;219(1):266-73.
- 483 17. Deng H, Dodson MW, Huang H, Guo M. The Parkinson's disease genes pink1 and parkin
484 promote mitochondrial fission and/or inhibit fusion in *Drosophila*. *Proc Natl Acad Sci USA*.
485 2008;105(38):14503-8.
- 486 18. Poole AC, Thomas RE, Andrews LA, McBride HM, Whitworth AJ, Pallanck LJ. The
487 PINK1/Parkin pathway regulates mitochondrial morphology. *Proceedings of the National Academy*
488 *of Sciences of the United States of America*. 2008;105(5):1638-43.
- 489 19. Yang Y, Ouyang Y, Yang L, Beal MF, McQuibban A, Vogel H, et al. Pink1 regulates
490 mitochondrial dynamics through interaction with the fission/fusion machinery. *Proc Natl Acad Sci*
491 *USA*. 2008;105(19):7070-5.
- 492 20. Park J, Lee G, Chung J. The PINK1-Parkin pathway is involved in the regulation of
493 mitochondrial remodeling process. *Biochem Biophys Res Commun*. 2009;378(3):518-23.
- 494 21. Burman JL, Yu S, Poole AC, Decal RB, Pallanck L. Analysis of neural subtypes reveals
495 selective mitochondrial dysfunction in dopaminergic neurons from parkin mutants. *Proceedings of*
496 *the National Academy of Sciences of the United States of America*. 2012;109(26):10438-43.
- 497 22. Vilain S, Esposito G, Haddad D, Schaap O, Dobрева MP, Vos M, et al. The yeast complex I
498 equivalent NADH dehydrogenase rescues pink1 mutants. *PLoS genetics*. 2012;8(1):e1002456.

- 499 23. Fernandes C, Rao Y. Genome-wide screen for modifiers of Parkinson's disease genes in
500 *Drosophila*. *Mol Brain*. 2011;4:17.
- 501 24. Pogson JH, Ivatt RM, Sanchez-Martinez A, Tufi R, Wilson E, Mortiboys H, et al. The Complex
502 I Subunit NDUFA10 Selectively Rescues *Drosophila pink1* Mutants through a Mechanism
503 Independent of Mitophagy. *PLoS genetics*. 2014;10(11):e1004815.
- 504 25. Giansanti MG, Belloni G, Gatti M. Rab11 is required for membrane trafficking and actomyosin
505 ring constriction in meiotic cytokinesis of *Drosophila* males. *Mol Biol Cell*. 2007;18(12):5034-47.
- 506 26. Giansanti MG, Farkas RM, Bonaccorsi S, Lindsley DL, Wakimoto BT, Fuller MT, et al.
507 Genetic dissection of meiotic cytokinesis in *Drosophila* males. *Mol Biol Cell*. 2004;15(5):2509-22.
- 508 27. Brill JA, Hime GR, Scharer-Schuksz M, Fuller MT. A phospholipid kinase regulates actin
509 organization and intercellular bridge formation during germline cytokinesis. *Development*.
510 2000;127(17):3855-64.
- 511 28. Plevoy G, Wei HC, Wong R, Szentpetery Z, Kim YJ, Goldbach P, et al. Dual roles for the
512 *Drosophila* PI 4-kinase four wheel drive in localizing Rab11 during cytokinesis. *J Cell Biol*.
513 2009;187(6):847-58.
- 514 29. Clark IE, Dodson MW, Jiang C, Cao JH, Huh JR, Seol JH, et al. *Drosophila pink1* is required
515 for mitochondrial function and interacts genetically with parkin. *Nature*. 2006;441(7097):1162-6.
- 516 30. Perkins LA, Holderbaum L, Tao R, Hu Y, Sopko R, McCall K, et al. The Transgenic RNAi
517 Project at Harvard Medical School: Resources and Validation. *Genetics*. 2015;201(3):843-52.
- 518 31. Godi A, Pertile P, Meyers R, Marra P, Di Tullio G, Iurisci C, et al. ARF mediates recruitment
519 of PtdIns-4-OH kinase-beta and stimulates synthesis of PtdIns(4,5)P₂ on the Golgi complex. *Nature*
520 *cell biology*. 1999;1(5):280-7.
- 521 32. Di Paolo G, De Camilli P. Phosphoinositides in cell regulation and membrane dynamics.
522 *Nature*. 2006;443(7112):651-7.
- 523 33. Nagashima S, Tabara LC, Tilokani L, Paupe V, Anand H, Pogson JH, et al. Golgi-derived
524 PI(4)P-containing vesicles drive late steps of mitochondrial division. *Science (New York, NY)*.
525 2020;367(6484):1366-71.

- 526 34. Vincow ES, Thomas RE, Merrihew GE, Shulman NJ, Bammler TK, MacDonald JW, et al.
527 Autophagy accounts for approximately one-third of mitochondrial protein turnover and is protein
528 selective. *Autophagy*. 2019;15(9):1592-605.
- 529 35. Vincow ES, Merrihew G, Thomas RE, Shulman NJ, Beyer RP, MacCoss MJ, et al. The
530 PINK1-Parkin pathway promotes both mitophagy and selective respiratory chain turnover in vivo.
531 *Proceedings of the National Academy of Sciences of the United States of America*.
532 2013;110(16):6400-5.
- 533 36. McWilliams TG, Prescott AR, Montava-Garriga L, Ball G, Singh F, Barini E, et al. Basal
534 Mitophagy Occurs Independently of PINK1 in Mouse Tissues of High Metabolic Demand. *Cell*
535 *metabolism*. 2018;27(2):439-49 e5.
- 536 37. Lee JJ, Sanchez-Martinez A, Zarate AM, Beninca C, Mayor U, Clague MJ, et al. Basal
537 mitophagy is widespread in *Drosophila* but minimally affected by loss of Pink1 or parkin. *J Cell Biol*.
538 2018;217(5):1613-22.
- 539 38. Whitworth AJ, Pallanck LJ. PINK1/Parkin mitophagy and neurodegeneration-what do we
540 really know in vivo? *Curr Opin Genet Dev*. 2017;44:47-53.
- 541 39. Kim YY, Um JH, Yoon JH, Kim H, Lee DY, Lee YJ, et al. Assessment of mitophagy in mt-
542 Keima *Drosophila* revealed an essential role of the PINK1-Parkin pathway in mitophagy induction in
543 vivo. *FASEB J*. 2019;33(9):9742-51.
- 544 40. Cornelissen T, Vilain S, Vints K, Gounko N, Verstreken P, Vandenberghe W. Deficiency of
545 parkin and PINK1 impairs age-dependent mitophagy in *Drosophila*. *Elife*. 2018;7.
- 546 41. Sandoval H, Yao CK, Chen K, Jaiswal M, Donti T, Lin YQ, et al. Mitochondrial fusion but not
547 fission regulates larval growth and synaptic development through steroid hormone production. *Elife*.
548 2014;3.
- 549

Supplementary Table 1. Details of full genotypes used in this study. More details of each line can be found in Methods.

Figure 1	
<u>Label</u>	<u>Genotype</u>
A	
Control	da-GAL4/+
fwd ³	fwd ³ /Df(3L)7C, da-GAL4
fwd ³ + fwd O/E	UAS-GFP-fwd/+; fwd ³ /Df(3L)7C, da-GAL4
fwd ^{neo1}	fwd ^{neo1} /Df(3L)7C, da-GAL4
fwd ^{neo1} + fwd O/E	UAS-GFP-fwd/+; fwd ^{neo1} /Df(3L)7C, da-GAL4
B	
Control	da-GAL4/+
fwd ³	fwd ³ /Df(3L)7C, da-GAL4
C	
Control	da-GAL4/+
fwd ³	fwd ³ /Df(3L)7C
D	
<u>Ubiquitous:</u>	
control-RNAi	da-GAL4/UAS-Luciferase-RNAi
fwd-RNAi	da-GAL4/UAS-fwd-RNAi
<u>Neuronal:</u>	
control-RNAi	nSyb-GAL4/UAS-Luciferase-RNAi
fwd-RNAi	nSyb-GAL4/UAS-fwd-RNAi
<u>Muscle:</u>	
control-RNAi	Mef2-GAL4/UAS-Luciferase-RNAi
fwd-RNAi	Mef2-GAL4/UAS-fwd-RNAi

Figure 2	
<u>Label</u>	<u>Genotype</u>
A	
Control	UAS-mito-HA-GFP/+; da-GAL4/+
fwd ³	UAS-mito-HA-GFP/+; fwd ³ /Df(3L)7C, da-GAL4
B	
Control	da-GAL4/+
fwd ³	fwd ³ /Df(3L)7C, da-GAL4
C-F	
Control	CCAP-GAL4,UAS-mito-Tomato/ UAS-mito-HA-GFP; fwd ³ /+
fwd ³	CCAP-GAL4,UAS-mito-Tomato/UAS-mito-HA-GFP; fwd ³ /Df(3L)7C

Figure 3	
<u>Label</u>	<u>Genotype</u>
A, B	
Control	da-GAL4/+
fwd ³	fwd ³ /Df(3L)7C, da-GAL4

Figure 4	
<u>Label</u>	<u>Genotype</u>
A	
Control	da-GAL4/UAS-mito-HA-GFP
fwd ^{RNAi}	da-GAL4/UAS-fwd-RNAi
Marf ^{-/+}	Marf ^B /w ¹¹¹⁸ ; da-GAL4/ UAS-mito-HA-GFP
Marf ^{-/+} ; fwd ^{RNAi}	Marf ^B / w ¹¹¹⁸ ; da-GAL4/UAS-fwd-RNAi

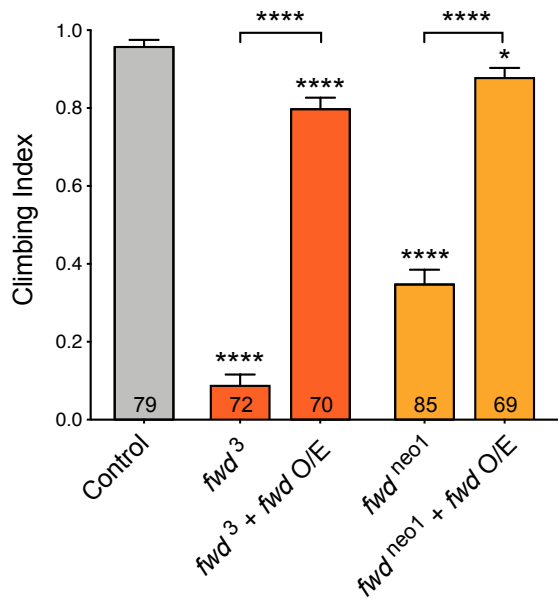
B	
Control	da-GAL4/ UAS-mito-HA-GFP
<i>fwd</i> ^{RNAi}	da-GAL4/UAS- <i>fwd</i> -RNAi
<i>Opa1</i> ^{-/+}	<i>Opa1</i> ^{s3475/+} ; da-GAL4/UAS-mito-HA-GFP
<i>Opa1</i> ^{-/+} ; <i>fwd</i> ^{RNAi}	<i>Opa1</i> ^{s3475/+} ; da-GAL4/UAS- <i>fwd</i> -RNAi
C	
Control	da-GAL4/+
<i>fwd</i> ^{RNAi}	UAS-mito-HA-GFP/+; da-GAL4/UAS- <i>fwd</i> -RNAi
Drp1 O/E	UAS-mito-HA-GFP/+; da-GAL4/UAS-Drp1
Drp1 O/E + <i>fwd</i> ^{RNAi}	da-GAL4/UAS- <i>fwd</i> -RNAi, UAS-Drp1
D	
Control	UAS-mito-HA-GFP/+; CCAP-GAL4/+
<i>fwd</i> ^{RNAi}	UAS-mito-HA-GFP/+; CCAP-GAL4/UAS- <i>fwd</i> -RNAi
<i>Marf</i> ^{-/+} , <i>fwd</i> ^{RNAi}	<i>Marf</i> ^{B/w¹¹¹⁸} ; UAS-mito-HA-GFP/+; CCAP-GAL4/UAS- <i>fwd</i> -RNAi
<i>Opa1</i> ^{-/+} , <i>fwd</i> ^{RNAi}	UAS-mito-HA-GFP/ <i>Opa1</i> ^{s3475} ; CCAP-GAL4/UAS- <i>fwd</i> -RNAi
Drp1 O/E + <i>fwd</i> ^{RNAi}	UAS-mito-HA-GFP/+; CCAP-GAL4/UAS- <i>fwd</i> -RNAi, UAS-Drp1

Figure 5	
<u>Label</u>	<u>Genotype</u>
A, C	
Control	da-GAL4/+
<i>fwd</i> O/E	UAS-GFP- <i>fwd</i> /+; da-GAL4/+
<i>park</i> ^{-/-}	<i>park</i> ²⁵ / <i>park</i> ²⁵ , da-GAL4
<i>park</i> ^{-/-} , <i>fwd</i> O/E	UAS-GFP- <i>fwd</i> /+; <i>park</i> ²⁵ / <i>park</i> ²⁵ , da-GAL4

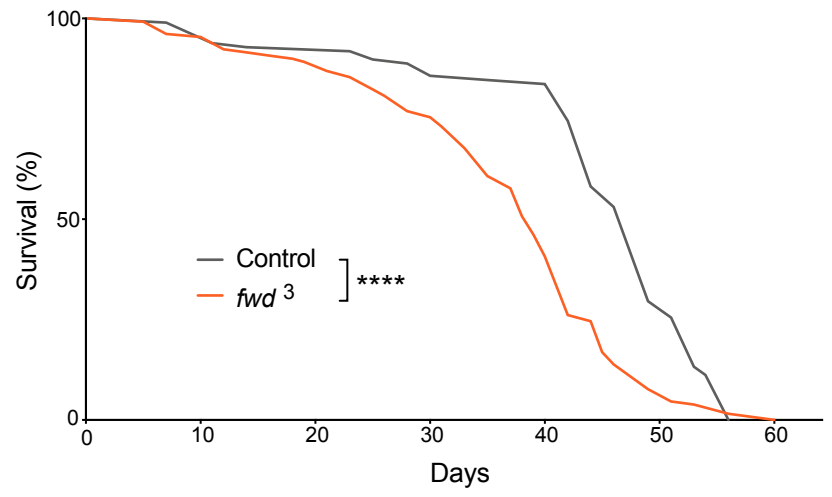
B, C	
Control	da-GAL4/+
fwd O/E	UAS-GFP-fwd/+; da-GAL4/+
Pink1 ⁻	Pink1 ^{B9} /Y; da-GAL4/+
Pink1 ⁻ , fwd O/E	Pink1 ^{B9} /Y; UAS-GFP-fwd/+; da-GAL4/+
D	
Control	UAS-mito-HA-GFP/+; Mef2-GAL4/+
Pink1 ⁻	Pink1 ^{B9} /Y; UAS-mito-HA-GFP/+; Mef2-GAL4/+
Pink1 ⁻ , fwd O/E	Pink1 ^{B9} /Y; UAS-GFP-fwd/+; Mef2-GAL4/+
park ^{-/-}	park ²⁵ / park ²⁵ , Mef2-GAL4
park ^{-/-} , fwd O/E	UAS-GFP-fwd/+; park ²⁵ / park ²⁵ , Mef2-GAL4

Figure 6	
<u>Label</u>	<u>Genotype</u>
A, C	
Control	UAS-mito-HA-GFP /+; da-GAL4/+
Pink1 ⁻	Pink1 ^{B9} /Y; UAS-mito-HA-GFP/+; da-GAL4/+
Pink1 ⁻ , Drp1 O/E	Pink1 ^{B9} /Y; UAS-mito-HA-GFP/+; da-GAL4/UAS-Drp1
Pink1 ⁻ , Drp1 O/E + fwd ^{RNAi}	Pink1 ^{B9} /Y; da-GAL4/UAS-fwd-RNAi, UAS-Drp1
B, D	
Control	UAS-mito-HA-GFP /+; da-GAL4/+
park ^{-/-}	park ²⁵ /park ²⁵ , da-GAL4
park ^{-/-} , Drp1 O/E	UAS-mito-HA-GFP/+; park ²⁵ , UAS-Drp1/park ²⁵ , da-GAL4
park ^{-/-} , Drp1 O/E + fwd ^{RNAi}	UAS-fwd-RNAi, park ²⁵ , UAS-Drp1/park ²⁵ , da-GAL4

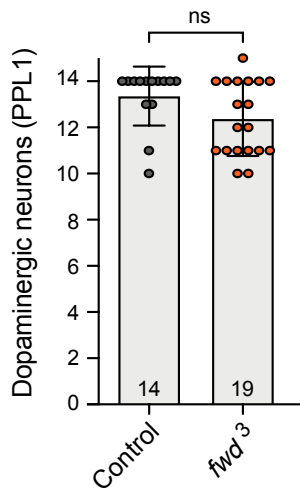
A



B



C



D

